Available online at www.sciencedirect.com
SCIENCE DIRECT
Journal of Crystal Growth 290 (2006) 6–10
JOURNAL OF CRYSTAL GROWTH
www.elsevier.com/locate/jcrysgro

Growth phenomena of Si and Si/Ge nanowires on Si (1 1 1) by molecular beam epitaxy

N.D. Zakharov, P. Werner*, G. Gerth, L. Schubert, L. Sokolov, U. Gösele

Max Planck Institute of Microstructure Physics, Weinberg 2, D-06120 Halle (Saale), Germany

Received 4 July 2005; accepted 21 December 2005
Available online 7 February 2006
Communicated by R.M. Biefeld

Abstract

We report on the formation of Si and SiGe nanowires (NW) by molecular beam epitaxy (MBE) initiated via gold droplets. The MBE growth behavior essentially differs from the classical vapor–liquid–solid mechanism (VLS) observed in the case of NW growth by chemical vapor deposition (CVD). From a thermodynamic point of view, the driving force for the NW growth by MBE is related to the supersaturation determined by relaxation of elastic energy generated in Si substrate due to Au intrusion. Adding Ge decreases the growth rate of Si NW or can even result in its dissolution. This effect can be interpreted in terms of elastic energy accumulation because of differences in atomic radii of Si and Ge. This effect has a general influence on the formation of NW heterostructures.

Keywords: A1. Nanostructures; A3. Molecular beam epitaxy; B1. Semiconducting silicon compounds

1. Introduction

There is an increasing interest in the formation of nanostructures and their physical properties, e.g., in the possibility to explore quantum size effects [1–4]. Nanowhiskers (NW, also referred to as nanowires) are one of these structures. Extensive investigations of the growth of silicon whiskers by the so-called "vapor–liquid–solid" (VLS) technique started already in the 1960s [5–8]. To initiate the formation of whiskers using the VLS mechanism, small liquid metal droplets are usually used as seeds. Further CVD growth occurs because of a high accommodation of the vapor-phase species/molecules/ad-atoms on the liquid surface of the Si/Au eutectic, where the reduction reaction, e.g., $SiCl_4 + 2H_2 = Si + 4HCl\uparrow$, occurs. The necessary supersaturation of Si ad-atoms is determined by the vapor pressure in the reaction chamber. The growth occurs entirely due to the adsorption of Si ad-atoms on the metal droplet. This growth process can also be used for the generation of nanowhiskers including SiGe heterostructures, which are interesting for new device concepts. Both the formation of vertically incorporated germanium layers [9] as well as radial germanium embedding [10] were successfully demonstrated. Pulse laser deposition (PLD) was used by Park and Hogan [11] to grow Si wires on a Si(1 1 1) substrate. Authors suggest that growth occured via well-known VLS mechanism.

Much less is known about the growth of Si nanowhiskers by molecular beam epitaxy (MBE). Also, NW heterostructures have been grown mainly by MOCVD, especially III–V NW, as demonstrated, e.g., in Ref. [12]. The MBE technique is characterized by a uniform flux of Si or Ge atoms impinging on the substrate surface. In this case small Au droplets previously deposited as seeds do not act as catalysts to crack precursor molecules (as it occurs in CVD), but absorb Si monomers to the same degree as the Si substrate surface does it. In that view both the Si layer as well as the Si whisker under the gold droplet should grow at the same speed. However, in the case of MBE whiskers grow much faster [13], as demonstrated by scanning electron microscopy (SEM, see Fig. 1). The aim of this paper is to provide a better insight into this specific MBE growth mechanism and the possibility to incorporate

*Corresponding author. Tel.: +49 345 5582629.
E-mail address: werner@mpi-halle.de (P. Werner).

0022-0248/$ - see front matter © 2006 Elsevier B.V. All rights reserved.
doi:10.1016/j.jcrysgro.2005.12.096

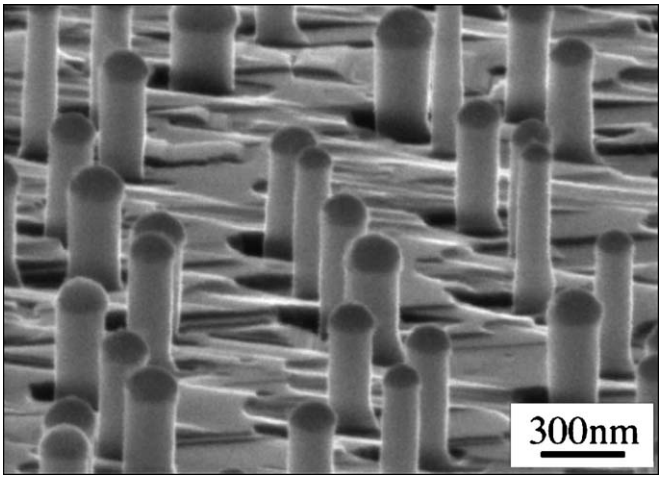

Fig. 1. SEM overview image of Si whiskers grown on a Si {1 1 1} substrate at $T_S = 525\,^{\circ}C$. The whiskers show a pillar shape and are capped by Au droplets (dark contrast). The wafer surface during the growth process is getting rough.

thin Ge layers into Si whiskers to form Si/Ge heterostructures.

2. Experiments

⟨1 1 1⟩ oriented 5″ Si wafers cleaned by the conventional RCA procedure were used as substrates. Our MBE system includes three electron-beam guns for the evaporation of Au and Si as well as of Ge [13]. A thin Au film with a nominal thickness of 2 nm was deposited on the substrate at a substrate temperature T_S of 525 °C. During the following NW growth the constant Si and Ge fluxes amounted to 0.05 and 0.01 nm/s, respectively. In this particular case of Si and Si/Ge whiskers, two growth temperatures T_S of (i) 525 °C and (ii) 545 °C were chosen. The samples were investigated by transmission electron microscopy (TEM) and high-resolution SEM. The Ge concentration was measured by many-beam TEM bright-field imaging. Fig. 1 gives a SEM overview image of such a structure, where the Si NWs have the morphology of pillars.

3. Results and discussion

Gold deposition results in formation of ensemble of small Au droplets on Si substrate where the droplet's size varied between 10 and 300 nm. Interaction of Au with the substrate (see (E) in Fig. 2(d)) results in an increase of the elastic energy in the surface layer. The presence of an Au-enriched surface layer has also been demonstrated in Ref. [14]. The gold-induced stress can be reduced at the top of NW since the constraint of the substrate lattice is no longer present. The stress in the surface layer of the substrate may even lead to the generation and movement of dislocations as was experimentally observed.

During the subsequent Si deposition, NWs are formed under the Au droplets (Fig. 2(a)). Their diameter d is

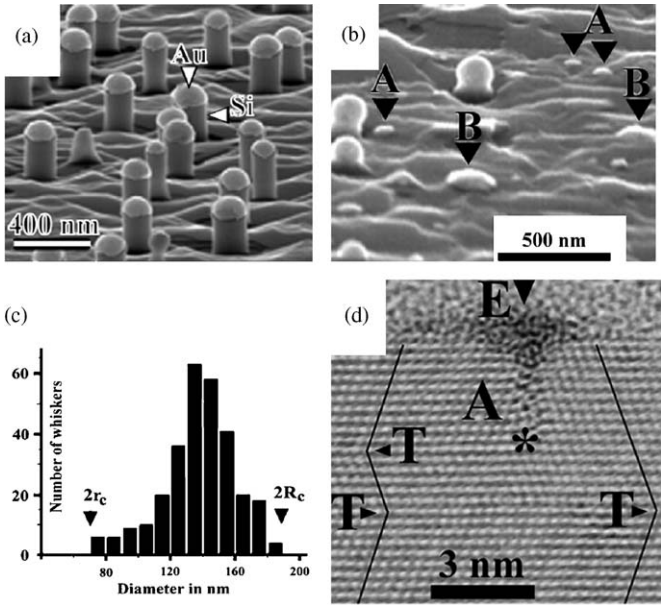

Fig. 2. (a) SEM image of whiskers grown at 525 °C for 2 h. Note that each whisker is surrounded by a trough in the substrate. (b) SEM image taken at the beginning of growth. Large Au droplets (B) as well as very small ones (A) do not initiate whisker growth. (c) Diameter distribution of the whiskers. (d) Intrusion of Si/Au eutectic (E) into substrate at (A) resulting in the formation of structural defects. T-twin boundaries, position of partial dislocation is marked by *.

related to the size of the droplet and varies in the range between 60 and 180 nm ($2r_c < d < 2R_c$) for the experimental conditions investigated. Smaller droplets as well as larger droplets outside of this range do not initiate a whisker growth at all (see arrows in Figs. 2(b) and (c)).

In the case of MBE whisker growth, two fluxes of Si ad-atoms can be distinguished as schematically shown in Fig. 3(b). The uniform flux I_1 comes directly from the Si source and provides the component of vertical elongation equal to the thickness of the overgrown Si layer L_s. The whole vertical elongation of the whisker amounts to $L + L_S$. The visible whisker length L is fully determined by flux I_2, which collects adsorbed Si ad-atoms from a region with a radius R_s around the whisker. The base of the whiskers is always found in triangular pits formed during the growth. This indicates that some surrounding silicon material is definitely consumed by the whisker (see Fig. 2(a)). Si atoms diffuse upward to the Au droplet and are incorporated into the (1 1 1) Si/Au droplet interface. This growth process implies the presence of an ad-atom supersaturation because of a gradient of the chemical potential $\Delta\mu > 0$ [15]:

$$\Delta\mu = \Delta\mu_0 - 2\Omega\gamma/R, \tag{1}$$

where $\Delta\mu_0 = \mu_s - \mu_w$ results from the difference of the chemical potentials between a Si atom on an Au-enriched surface layer of the substrate (μ_s) and a Si atom at the top of the whisker (μ_w, see also Fig. 3). The first term in Eq. (1) is positive since $\mu_s > \mu_w$ because of the elastic energy relaxation in the whisker (see Fig. 3(c)). In the second term,

R denotes the whisker's radius, Ω the atomic volume, and γ the surface energy. This term reduces the supersaturation $\Delta\mu/kT$ due to the increasing of surface energy and imposes limitations on the smallest whisker radius, which can still grow. For the whiskers with radius r_c, the supersaturation vanishes ($\Delta\mu/k = 0$) and the growth stops. This behavior is referred to as the Gibbs–Tompson effect. Fig. 2(b) shows small Au droplets marked by A, which do not initiate a whisker growth. Under our experimental conditions we found a r_c of about 35 nm (Fig. 2(c)).

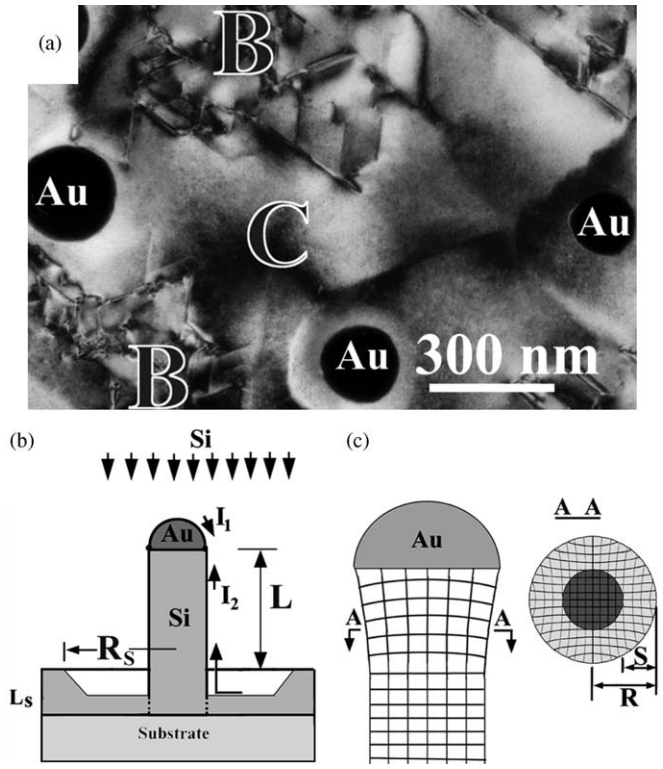

Fig. 3. (a) TEM plan-view image of initial stage of whisker growth. Whiskers start grow under Au caps (black circles). B—dislocated areas. Notice that structural defects, serving for stress relaxation, are absent in the vicinity of growing whiskers. (b) Schematic representation of MBE whisker growth. I1, I2- fluxes of Si ad-atoms directed to gold cap. (c) Schematic representation of elastic energy relaxation in the whisker.

TEM images reveal a high density of tiny (about 3 nm in size) droplets of Si/Au eutectic on the Si surface. One of this droplet E is shown in Fig. 2(d). They have amorphous structure and are definitely liquid at growth temperature. One can see that intrusion of Au into substrate results in structural defects formation such as twins T and partial dislocations A. Thus, interaction of these tiny droplets with the silicon surface increases stress state in a gold-enriched Si surface layer. This elastic energy may be reduced by formation of thin pillars, where the crystal lattice does not any longer constrained. The related relaxation of the crystal lattice in a small pillar is schematically shown in Fig. 3(c). In this particular cross-section scheme, a whisker close to its tip contains two areas: (i) the central region (dark) with the chemical potential being nearly equal to the chemical potential in the substrate, and (ii) the relaxed outer region (bright) with a potential μ_{rel} ($\mu_{rel} < \mu_s$). In this case the gain of the chemical potential supplied by strain relaxation is a function of geometry (R, S) and decreases with an increasing radius R. The supersaturation supplied by strain relaxation can be written:

$$\Delta\mu_0 = \mu_{sub} - \mu_{rel} - (\mu_{sub} - \mu_{rel})(R - S)^2/R^2. \quad (2)$$

In the case of thin whisker $R = S$ (full relaxation), we will get highest supersaturation $\Delta\mu_0 = \mu_{sub} - \mu_{rel}$. In the other extreme case $R \gg S$ gives $\Delta\mu_0 = 0$. This simple example qualitatively explains why thick whiskers with $R > R_c$ do not grow. It is well established that in the case of CVD silicon whiskers growth such an upper critical radius does not practically exist since whiskers with diameters in the millimeter range can be successfully grown [15].

In order to investigate the influence of stress effects, we incorporated Ge layers into the Si whiskers. As an example, three thin Ge layers with a thickness of 0.5, 1 and 1.5 nm, respectively, were deposited during the whisker growth (see Fig. 4(a)). During the Ge layer deposition the Si flux was interrupted. The corresponding concentration profile ($Si_{1-x}Ge_x$) measured along C–D in the whisker is shown in Fig. 4(b). Two results are obvious: (i) The Ge layers show a triangular concentration profile. The half-width of the Ge/Si peaks in the whisker (C–D)

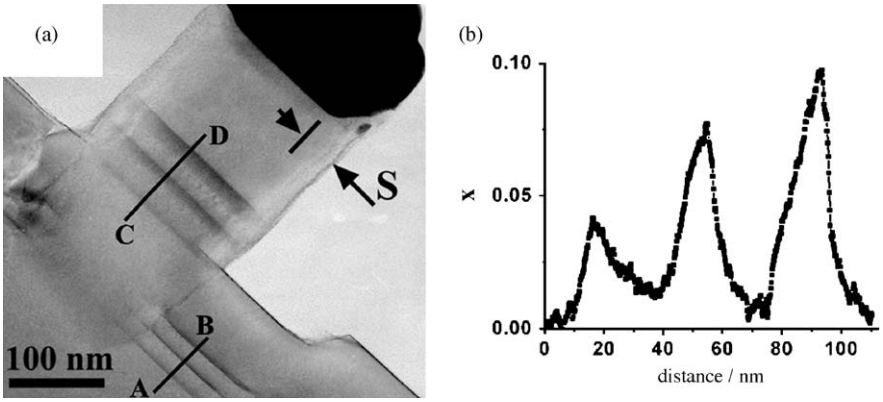

Fig. 4. (a) TEM image of whisker with three Ge layers. (b) Ge concentration profile measured along C–D.

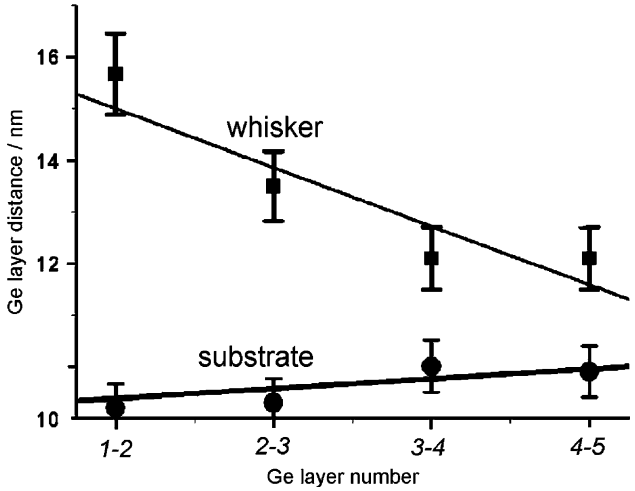

Fig. 5. Results of a Ge markers experiment to measure the growth rate of the whisker and adjacent substrate layer. In this experiment 5 Ge layers were incorporated. The Si spacer thickness between adjacent Ge layers ($n-m$) was measured.

is approximately 10 times larger than the nominally deposited Ge thickness. (ii) The Ge incorporation increases with a specific gradient. In general, the concentration x in the layers is relatively low. It starts from $x = 0.04$ ($= 4\%$) in the first layer and reaches $x = 0.10$ in the third layer.

These two facts demonstrate the problem of the MBE growth of vertical Ge layers in a Si whisker with an atomically sharp interface. It seems that Ge can be incorporated in the whisker matrix only as a Si-rich alloy, which might be caused by the Si/Ge lattice misfit. The Ge incorporation behavior in the surrounding Si layer is different (see A–B). Here we observed sharp peaks, where the Ge concentration reached values up to $x = 0.25$. Such values are known from the growth of Si/Ge quantum wells.

How does the incorporation of Ge influence the growth of the Si whisker? The growth speed of Si can be investigated by experiments using Ge marker layers similar to what is shown in Fig. 4. Such an experiment is represented in Fig. 5. In this case 5 thin Ge layers (each 1 nm) were incorporated in a Si whisker to measure the distances between them; e.g., 2–3 means the distance between the 2nd and 3rd Ge layer. The nominal Si spacer between the Ge layers amounted to 10 nm. In the Si layer overgrown on the substrate the Si spacer amounts to 10 nm within the error bar, however, in the whisker the incorporated Si spacer is decreasing from 15 to 12 nm. We suppose that the incorporation of Ge results in an accumulation of elastic energy in the whisker and a corresponding decrease of supersaturation. Therefore, the rate of incorporated Si is reduced with increasing of Ge content.

The deposition of a larger amount of Ge can even result in dissolution of the previously grown Si whiskers as observed experimentally (negative growth rate, $\Delta\mu < 0$). This phenomenon can be explained in the following manner: In the case of foreign atoms incorporation the supersaturation $\Delta\mu/kT$ can be written by

$$\Delta\mu/kT = (\Delta\mu_0 - 2\omega\gamma/R - \Delta\mu_e)/kT, \quad (3)$$

where $\Delta\mu_e$ denotes the elastic distortions due to the incorporation of the foreign atoms with different atomic radii. It is given by [16,17]

$$\Delta\mu_e = 9x\omega G\varepsilon^2, \quad (4)$$

where x denotes the concentration of Ge in atomic fractions, G the shear modulus, $\varepsilon = (r_m - r_i)/r_m$ the atomic misfit parameter, and r_m and r_i denote the atomic radii of the matrix and the impurity (Ge), respectively. For the given parameters $\Delta\mu_e$ amounts to $\sim 0.2x$ eV/atom. Hence, there is a critical Ge concentration x_c when the supersaturation $\Delta\mu$ reaches zero. This stops the whisker growth. We observed a growth interruption for $x_c = 0.05$, which would correspond to $\Delta\mu_e = 0.01$ eV. This result demonstrates that without Ge incorporation whisker growth occurs at a supersaturation of about $\Delta\mu_e/kT \approx 0.15$. This value is in a good agreement with data given by Givargizov [7]. Thus, the Ge doping can be used as a tool to measure supersaturations. Let us point out again that a similar effect of growth suppression due to Ge incorporation has not been reported in the case of CVD Si whisker growth [9].

4. Conclusion

MBE has been successfully applied to grow Si nanowhiskers and Si/Ge nanowhisker heterostructures. We found out that driving force for the MBE whisker growth is associated with the difference in the chemical potential of silicon atoms incorporated in a gold-enriched surface layer on the wafer surface and at the top of the silicon nanowhisker and especially at the rim of the tip where elastic relaxation can occur. In contrast to the conventional VLS mechanism, where the supersaturation of ad-atoms can be varied in a wide range due to $SiCl_4$ or SiH_4 gas pressure, in the case of MBE the supersaturation appears not to be an independent parameter which can be varied easily by simply changing the deposition rates. The radius of MBE grown whiskers vary in the case of the particular chosen growth temperature of 525 °C in a rather small interval of 35–100 nm. The smallest radius of the whiskers is determined by the Gibbs–Tompson effect, while the largest radius of whiskers appears to be determined by the ratio of relaxed/nonrelaxed volumes. The incorporation of Ge into Si nanowhisker leads to elastic energy accumulation, which may even prevent further whisker growth. We are presently investigating whether modifications of the silicon surface (hydrogen coverage or contamination by oxygen or carbon) allow us to decrease the lower critical radius into the 10 nm range under MBE growth conditions.

References

[1] Y. Nakajiama, Y. Takahashi, S. Horiguchi, K. Iwadate, H. Namatsu, K. Kurihara, M. Tabe, Appl. Phys. Lett. 65 (1994) 2833.

[2] N. Usami, T. Mine, S. Fukatsu, Y. Shiraki, Appl. Phys. Lett. 64 (1994) 1126.
[3] J.L. Liu, Y. Shi, F. Wang, Y. Lu, R. Zhang, P. Han, S.L. Gu, Y.D. Zheng, Appl. Phys. Lett. 68 (1996) 352.
[4] C.M. Lieber, MRS Bull. 28 (2003) 128.
[5] R.S. Wagner, W.C. Ellis, K. Jackson, S.M. Arnold, J. Appl. Phys. 35 (1964) 2993.
[6] R.S. Wagner, W.C. Ellis, Trans. Metall. Soc. AIME 233 (1965) 1053.
[7] E.I. Givargizov, J. Crystal Growth 31 (1975) 20.
[8] R.S. Wagner, W.C. Ellis, Appl. Phys. Lett. 4 (1964) 89.
[9] Y. Wu, R. Fan, P. Yang, Nano Lett. 2 (2002) 83.
[10] L.J. Lauhon, M.S. Gudiksen, D. Wang, C.M. Lieber, Nature 420 (2002) 57.
[11] H.D. Park, T.P. Hogan, J.Vac. Sci. Technol. B 22 (2004) 237.
[12] C.P.T. Svenson, W. Seifert, M.W. Larsson, L.R. Wallenberg, J. Stangl, G. Bauer, L. Samuelson, Nanotechnology 16 (2005) 936.
[13] L. Schubert, P. Werner, N.D. Zakharov, G. Gerth, F. Kolb, L. Long, U. Gösele, T.Y. Tan, Appl. Phys. Lett. 84 (2004) 4968.
[14] S. Takeda, K. Ueda, N. Ozaki, Y. Ohno, Appl. Phys. Lett. 82 (2003) 979.
[15] E.I. Givargizov, in: M. Senechal (Ed.), Highly Anisotropic Crystals, D. Reidel Publishing Company, Boston, 1987, p. 101.
[16] N.F. Mott, F.R.N. Nabarro, Proc. Phys. Soc. 52 (1940) 86.
[17] F.R.N. Nabarro, Proc. Roy. Soc. A 175 (1940) 519.